OPEN

Light: Science & Applications (2017) 6, e17095; doi:10.1038/lsa.2017.95
Official journal of the CIOMP 2047-7538/17
www.nature.com/lsa

ORIGINAL ARTICLE

Two-color multiphoton *in vivo* imaging with a femtosecond diamond Raman laser

Evan P Perillo[1], Jeremy W Jarrett[1], Yen-Liang Liu[1], Ahmed Hassan[1], Daniel C Fernée[1], John R Goldak[2], Andrei Bonteanu[1], David J Spence[3], Hsin-Chih Yeh[1] and Andrew K Dunn[1]

Two-color multiphoton microscopy through wavelength mixing of synchronized lasers has been shown to increase the spectral window of excitable fluorophores without the need for wavelength tuning. However, most currently available dual output laser sources rely on the costly and complicated optical parametric generation approach. In this report, we detail a relatively simple and low cost diamond Raman laser pumped by a ytterbium fiber amplifier emitting at 1055 nm, which generates a first Stokes emission centered at 1240 nm with a pulse width of 100 fs. The two excitation wavelengths of 1055 and 1240 nm, along with the effective two-color excitation wavelength of 1140 nm, provide an almost complete coverage of fluorophores excitable within the range of 1000–1300 nm. When compared with 1055 nm excitation, two-color excitation at 1140 nm offers a 90% increase in signal for many far-red emitting fluorescent proteins (for example, tdKatushka2). We demonstrate multicolor imaging of tdKatushka2 and Hoechst 33342 via simultaneous two-color two-photon, and two-color three-photon microscopy in engineered 3D multicellular spheroids. We further discuss potential benefits and applications for two-color three-photon excitation. In addition, we show that this laser system is capable of *in vivo* imaging in mouse cortex to nearly 1 mm in depth with two-color excitation.
Light: Science & Applications (2017) **6,** e17095; doi:10.1038/lsa.2017.95; published online 17 November 2017

Keywords: microscopy; nonlinear processes; three-dimensional imaging; ultrafast lasers

INTRODUCTION

Two-photon excitation (2PE) fluorescence microscopy is a widely used tool in neuroscience and biology for three-dimensional (3D) imaging of intact live specimen at the millimeter spatial scale with submicron resolution[1,2]. Implementing 2PE with commonly used fluorescent dyes and proteins is readily accomplished with femtosecond titanium-doped sapphire (Ti:S) lasers emitting in the range of 700–1000 nm. Unfortunately, the restricted wavelength tuning range of Ti:S lasers often leads to compromises in excitation efficiency with multicolor imaging experiments. Optimal excitation of fluorescent labels is even more critical when coupling 2PE with functional techniques such as Ca^{2+} imaging[3–5], pO_2 mapping[6–8], and optogenetics[9], where the probe selection is restricted. In addition, many of the recently developed fluorescent proteins (for example, mKate2, tdKatushka2, mNeptune, mCardinal) that offer exceptional brightness, long emission wavelength and photostability[10–12] have their 2PE peaks at longer wavelengths (1050–1200 nm), which enables deeper imaging in tissues[13,14]. It has recently been shown that a 50–100% improvement in imaging depth can be obtained by using 1050–1700 nm excitation, as compared with 800 nm excitation[15,16].

Excitation of multiple far-red fluorophores and functional probes (Ca^{2+}, pO_2 and optogenetic probes), which cover a broad spectral range presents a significant instrumentation challenge that cannot be achieved by a single Ti:S laser. Attempts to expand the palette of useable fluorophores have primarily relied on multiplexing excitation wavelengths through either discrete lasers[17] or with supercontinuum sources[18,19]. However, in the case of discrete lasers, the approach often involves an optical parametric oscillator (OPO) pumped by a Ti:S laser (1100–1600 nm), which is costly to implement, making this approach not available to many labs. While supercontinuum sources (600–1200 nm) are cheaper and provide flexible excitation wavelengths, they typically offer even lower power in a given spectral band (<10 mW), making these sources not suitable for deep tissue imaging.

Recently, an integrated and synchronized Ti:S laser and OPO system was used to perform both two-photon (2PE) and two-color two-photon (2C2P) excitation[20], enabling simultaneous excitation of three distinct fluorophores spread over a 250 nm-wide spectral region (850, 960 and 1100 nm). However, this Ti:S-OPO system only demonstrated shallow tissue imaging (~375 μm) in *ex vivo* samples[20,21]. If it were to be used for *in vivo* microscopy it would likely be limited to shallow depths because of the relatively short wavelength of the Ti:S imaging source. Furthermore, the high cost of the entire system may prevent its widespread use in the community. We believe the 2C2P excitation approach holds great promise for future deep, multicolor tissue imaging, as long as we can develop a low-cost home-built multicolor excitation system with a longer wavelength coverage (1050–1240 nm).

[1]Department of Biomedical Engineering, The University of Texas at Austin, TX 78712, USA; [2]Department of Physics, The University of Texas at Austin, TX 78712, USA and [3]MQ Photonics, Department of Physics and Astronomy, Macquarie University, Sydney, NSW 2109, Australia
Correspondence: AK Dunn, Email: adunn@utexas.edu
Received 21 December 2016; revised 22 May 2017; accepted 31 May 2017; accepted article preview online 1 June 2017

Here we demonstrate that such a low-cost multicolor excitation system can be built from a home-built high-powered ytterbium fiber amplifier and a home-built diamond Raman laser (Figure 1). Diamond Raman lasers offer a promising alternative to the Ti:S pumped OPO for two-color excitation microscopy, as they are inherently dual output through synchronous pumping, relatively low cost, have a simple cavity design, and require no active cooling or phase matching within their crystal[22,23]. Murtagh *et al.* have demonstrated that a Ti:S-pumped diamond Raman laser can achieve a significant Raman shift of ~90 nm (from 796 to 890 nm), proving a window large enough for two-color excitation[23]. However, this study was focused more on the characteristics of diamond Raman lasers and not their application to microscopy. To date, diamond Raman lasers have seen little use in microscopy. A Ti:S pumped diamond Raman laser has been used for asynchronous multi-color imaging in thin cell samples[24], and a Nd:YVO_4-pumped, picosecond diamond Raman laser emitting at 1240 nm has been demonstrated[25], but not used for imaging. We show, for the first time, that a diamond Raman laser can generate femtosecond (~100 fs) pulse-widths at 1240 nm through pumping with an amplified ytterbium fiber source, and that the output is stable enough for routine use as a microscopy source. In our system, the two synchronized and non-tunable output wavelengths for 2PE are centered at 1055 nm (λ_1) and 1240 nm (λ_2), provided by the ytterbium fiber amplifier and diamond Raman laser, respectively. Excitation at an effective wavelength of 1140 nm ($\lambda_3 = 2/(1/\lambda_1+1/\lambda_2)$) is achieved by spatiotemporal overlap of the two synchronized lasers (that is, 2C2P). We have significantly extended the capabilities of two-color excitation for deep *in vivo* imaging, as our integrated fiber-diamond laser system offers sufficiently high output power (>500 mW at 1055 nm, >300 mW at 1240 nm) and more suitable excitation coverage for far-red fluorescent proteins and dyes compared with a Ti:S pumped OPO (Figure 2). Despite the system's lack of wavelength tuning, we still achieve simultaneous 2P excitation of fluorophores over the broad range of 1000–1300 nm. Here we demonstrate deep *in vivo* imaging to nearly 1 mm in a mouse brain with 2C2P excitation (1140 nm) of Texas Red perfused vasculature, which is a 20% depth increase when compared with 1055 nm excitation. Interestingly, when performing simultaneous multicolor imaging of Hoechst 33342 and tdKatushka2 within an engineered 3D tumor spheroid model, we found that Hoechst 33342 was excited by an unexpected two-color three-photon (2C3P) process, while tdKatushka2 was excited by the expected 2C2P process. To our knowledge this is the first demonstration of a 2C3P excitation process for microscopy. The system cost is only about one-tenth that of a Ti:S-OPO system or commercial dual-output laser.

MATERIALS AND METHODS

Dual output laser system

The custom-built dual output laser system consists of a ytterbium fiber amplifier (Figure 1a) and diamond Raman laser (Figure 1b). The ytterbium fiber amplifier acts as both a source for imaging and a pump for the diamond Raman laser, therefore it is required to have sufficient output power, ~3 W, while still maintaining femtosecond pulse-widths, and high beam quality (Supplementary Fig. S1). We adopt an amplifier design that utilizes a single pass through large-mode-area fiber with input seed pulse parameters selected such that parabolic pulse evolution occurs[26,27]. In the parabolic amplification regime, nonlinear spectral broadening is balanced by normal dispersion. As a result, the pulse acquires only a linear chirp, even through several meters of fiber, which is easily compensated by standard grating or prism compressors. Parabolic pulse amplifiers have been built with output powers as high as 10 W and pulses as short as sub-100 fs[28–30]. Here, a fiber core size was selected to achieve the target

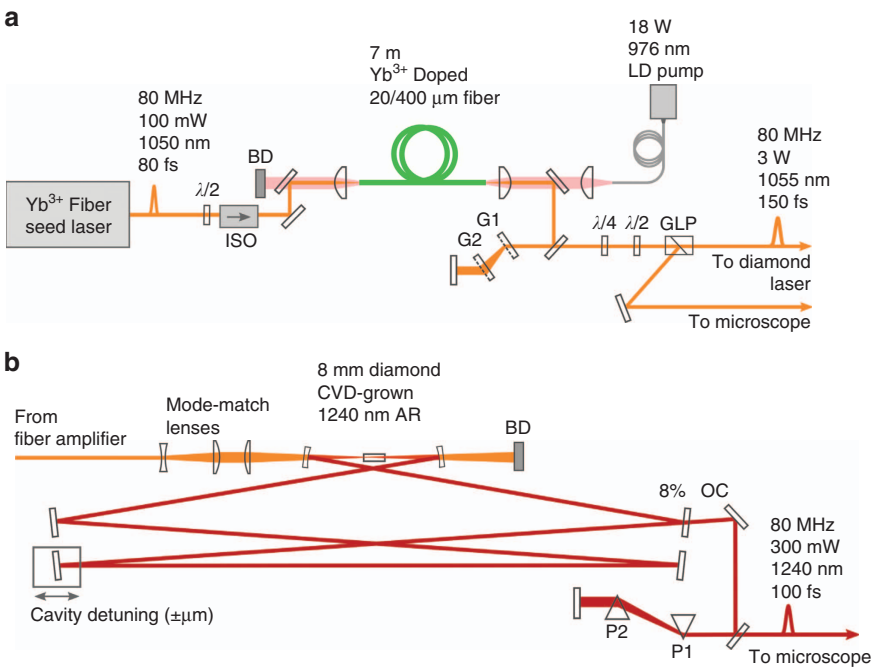

Figure 1 Laser system schematic. (**a**) Custom-built ytterbium fiber amplifier seeded by a commercial fiber oscillator. The amplified output is 3 W at 1055 nm with a pulse-width of 120 fs (**b**) Custom-built diamond Raman laser. The output is 300 mW at 1240 nm with a pulse-width of 100 fs. ISO is isolator, BD is beam dump, GLP is Glan-laser polarizer, G1 and G2 are transmission gratings, OC is output coupler, P1 and P2 are equilateral prisms, CVD is chemical vapor deposition.

doi:10.1038/lsa.2017.95

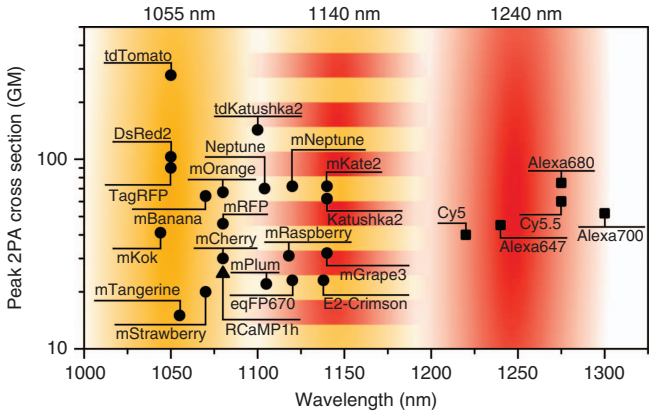

Figure 2 Efficient excitation of far-red fluorophores with fiber-pumped diamond Raman laser. A compilation of peak two-photon absorption cross sections from published literature[5,11,49]. The triangle is from Ref. 5, circles are from Ref. 11, and squares are from Ref. 49. The three wavelength bands of the dual output laser system shown overlaid on the graph, 1240 nm diamond Raman laser (red), 1055 nm ytterbium fiber amplifier (orange), and 1140 nm 2C2P excitation (striped). The laser system offers simultaneous and complete excitation coverage for fluorophores within the range of 1000–1300 nm.

requirement of 3 W output power (Supplementary Fig. S2). The amplifier is seeded with 50 mW from a commercial oscillator (Origami-10, OneFive GmbH), amplified up to 3 W, and the output pulses are compressed with an external grating pair to 120 fs. The emission wavelength is 1055 nm with a repetition rate of 80 MHz. For details on the amplifier setup, see Materials and methods section in Supplementary Information.

The diamond Raman laser is based on a ring cavity design according to previous embodiments[23,25], but with two differences. First, the cavity has two additional fold mirrors to maintain a footprint of <1 m in length, due to space constraints. Second, the ytterbium fiber amplifier pump is unique to this embodiment, and, to our knowledge, is the first demonstration using femtosecond pumping centered at 1055 nm to achieve a first Stokes Raman output at 1240 nm. The pump light is expanded with a telescope lens pair ($M=3$), and then focused ($fl=200$ mm) to achieve a mode-radius, $\omega_0=20$ μm, within the center of the diamond. The mirrors within the cavity are high reflectors ($R>99.5\%$) at 1240 nm, except for the output coupler, which has a transmission of ~8% at 1240 nm. Two curved mirrors with radius of curvature 200 mm focus the light into the diamond crystal. A diamond (CVD-grown, 8 mm long, 1240 nm AR-coating) with $<111>$ crystal axis aligned to the horizontal pump polarization generates the stimulated Raman gain. A cavity mirror mounted on a high precision flexure stage with integrated piezo drive (KPZNFL5, Thorlabs) allows matching of the cavity round trip time to the repetition rate of the pump for optimal overlap between pump and Stokes pulses within the crystal. The Stokes pulses that exit the cavity through the output coupler have a slight chirp, 400 fs, from the dispersion introduced by the diamond in the cavity. Using a pair of prisms (P1 and P2, in Figure 1b) the pulse width can be compressed down to 100 fs (Figure 3c).

Laser system characterization

The fiber amplifier and diamond laser pulse-widths were measured using an *in situ* autocorrelation technique with a GaAsP photodiode[31]. The benefit of *in situ,* over standalone, autocorrelation is that the exact pulse-width can be measured through the microscope objective used for imaging (25×, 1.0 NA, XLPN25XSVMP, Olympus). With this approach, the optimum pulse-width at the focal plane is achieved for both lasers, despite travelling through a highly dispersive objective lens. The minimum pulse-width of the fiber amplifier at the focus of the objective was found to be 120 fs (Figure 3a), although the pulse is affected by significant third-order dispersion (TOD), as evidenced by the secondary peak ~200 fs from the central pulse. The high TOD is caused by a combination of the amplification fiber, objective lens and pulse compression gratings. Without passing through the objective, it is possible to obtain a cleaner 120 fs pulse with no side lobes. Although the pulse distortion is not a significant limitation for this application, the use of shorter amplification fiber and prisms rather than gratings for compression would likely reduce the TOD significantly.

Interestingly, the diamond Raman laser autocorrelation (Figure 3c) is both cleaner and more compressed (100 fs), despite being pumped by the structured pulse from the fiber amplifier. The optimized Raman laser predominantly converts the long-wavelength components of the pump spectrum, with the central 1240 nm wavelength of the Stokes pulse corresponding to the longer-wavelength 1064 nm peak of the structured pump spectrum. This selective Raman conversion process along with self- and cross-phase modulation of the Stokes pulse itself results overall in a Stokes spectrum that is narrower than the 120 fs non-transform-limited pump pulse; however, the Stokes spectrum has less phase noise resulting in a shorter 100 fs Stokes pulse (Figure 3d), closer to its transform limit. We find that the fiber amplifier pulse-width affects the Raman conversion efficiency and resulting output power. To achieve the shortest 2C2P pulse, the fiber amplifier pulse-width was minimized at the objective focus, rather than at the focus of the diamond crystal. The optimization of the fiber amplifier pulse at the objective focus resulted in a small (~10%) decrease in output power from the diamond Raman laser. An ideal future solution would be independent compressors for both the pump and imaging paths of the fiber amplifier.

In addition to autocorrelation of individual laser pulses, we perform cross-correlation between both lasers to evaluate the effective 2C2P pulse-width (Figure 3b). The resulting full-width-half-max (FWHM) pulse-width was measured to be 220 fs. As expected, the cross-correlation shows that the effective 2C2P pulse-width is roughly equal to the temporal overlap between both excitation pulse-widths. The asymmetrical effect of TOD on the pulse due to the contribution from the fiber amplifier can clearly be seen from the cross-correlation.

Two-color multiphoton microscope

A custom-built upright microscope was used for all imaging experiments (Figure 4a). The fiber amplifier was routed through a delay line before being combined with the diamond laser with a shortpass dichroic mirror (alignment details discussed in Materials and methods section in Supplementary Information). The delay line is mounted on a motorized stage to perform cross-correlation measurements, and allow synchronization of the pulses during imaging experiments. After the pulses are combined onto a single optical axis, they enter the custom-built microscope stage.

The brightness enhancement afforded by 2C2P is noticeable when the pulses are delayed by several hundred femtoseconds ($\tau=\pm330$ fs) versus perfectly overlapped ($\tau=0$ fs) in a cell expressing tdKatushka2 (Figure 4b). The modulation depth of the brightness enhancement was quantified by recording the average signal in the image at varying pulse synchronization delays, τ (Figure 4c). A large modulation depth can be achieved for fluorophores with a small direct excitation cross-section (one-color two-photon, 1C2P), but high 2C2P cross-section. For a fluorophore with zero excitation cross-section at either 1C2P

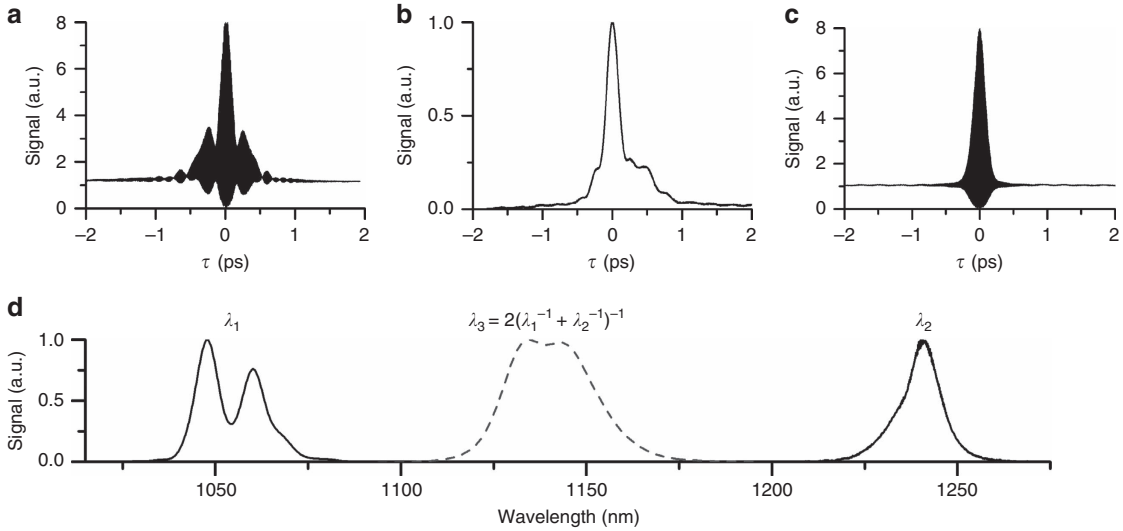

Figure 3 Laser characterization (**a**) Fiber amplifier autocorrelation, the pulse-width is 120 fs assuming a sech^2 pulse shape, (**b**) Cross-correlation between fiber amplifier and diamond Raman laser, the pulse width is 220 fs, estimated to be 110 fs after decorrelation. (**c**) Diamond Raman laser autocorrelation, the pulse-width is 100 fs assuming a sech^2 pulse shape. (**d**) Measured and calculated spectra of the fiber amplifier, diamond Raman laser, and effective 2C2P excitation. The 2C2P spectra were calculated from a cross-correlation of the measured fiber amplifier and diamond laser spectra.

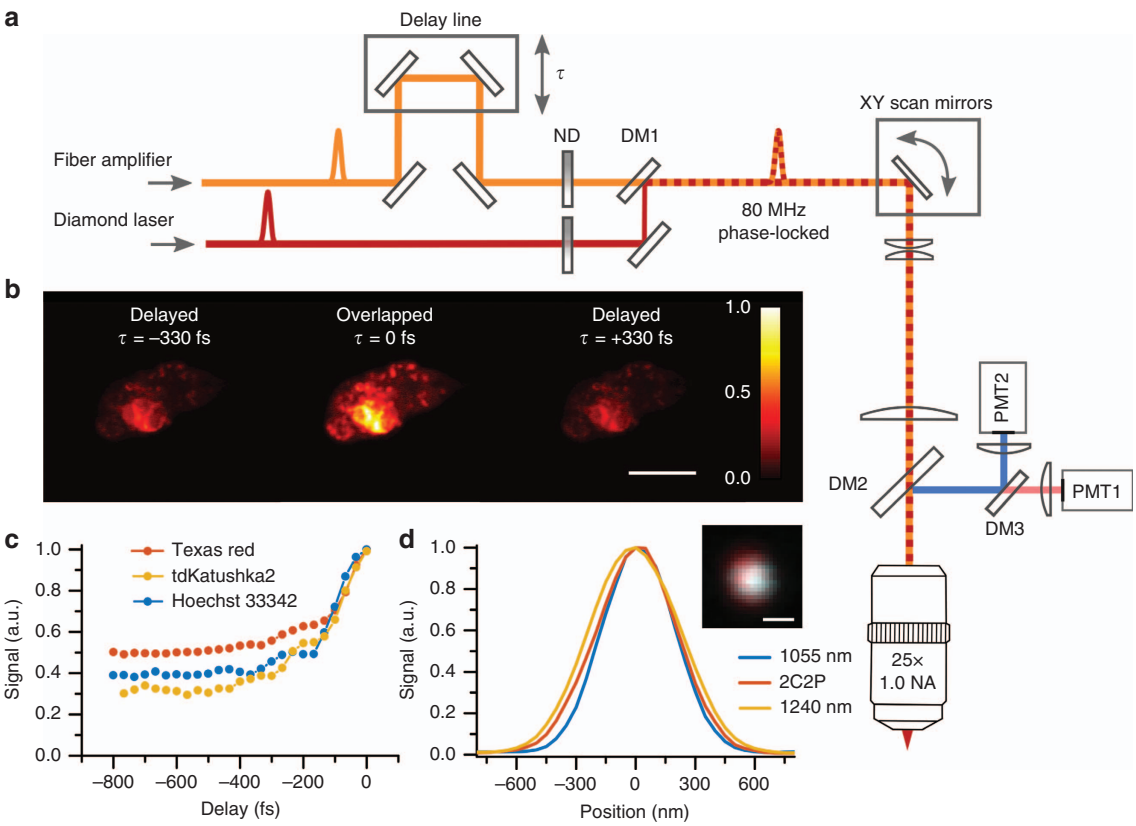

Figure 4 Two-color excitation microscope (**a**) Microscope schematic, the fiber amplifier is overlapped in time (τ) relative to the diamond Raman laser using a mirror delay line. Their ratio of excitation power is adjusted using independent neutral density filters (ND). Both pulses are sent into a custom-built two-photon upright microscope. (**b**) 2C2P excitation demonstrated on a single cell expressing tdKatushka2-VASP-5 at various pulse synchronization delay times, scale bar is 10 μm. (**c**) 2C2P excitation as a function of delay time, τ, for various fluorescent labels. (**d**) The point spread function line profiles for 1055 nm, 1240 nm and 2C2P excitation on 200 nm red fluorescent beads in agarose (inset: image of a single 200 nm bead with 1055 and 1240 nm excitation overlaid in blue and red respectively, scale bar is 500 nm). DM1 is a shortpass dichroic filter with edge at 1180 nm. DM2 and DM3 are longpass dichroic filters with edges at 775 and 570 nm, respectively.

doi:10.1038/lsa.2017.95

wavelength and non-zero excitation efficiency with 2C2P, the modulation depth approaches unity[20]. In the case of the fluorophores used here, the modulation ranges from 0.7 for tdKatushka2, to 0.5 for Texas Red. Additionally, it is possible to tune the modulation depth by adjusting the ratio of excitation powers (Supplementary Fig. S3). The point spread function (PSF) of each excitation regime was measured using 200 nm fluorescent microspheres (F8810, ThermoFisher) embedded in agarose (Figure 4d). The FWHM PSF lateral size was found to be 528, 602, and 635 nm, for $\lambda_1 = 1055$ nm, $\lambda_3 = 1140$ nm (2C2P), and $\lambda_2 = 1240$ nm, respectively.

RESULTS AND DISCUSSION

Two-color, three-photon excitation in spheroids

We evaluate 2C2P excitation by performing a multicolor imaging experiment in a spheroid of MCF-10A breast cancer cells. The spheroid, commonly used as a cancer tumor model, is a cluster of hundreds of cells arranged in 3D with dimensions of approximately $400 \times 400 \times 200\ \mu m^3$ (Supplementary Fig. S4). Multicolor imaging of two spectrally distinct labels is performed through transient expression of a fusion protein of vasodilator-stimulated phosphoprotein (VASP) with tdKatushka2 within the cytoplasm, and staining with Hoechst 33342 in the nucleus (Figure 5a). The effect of pulse delay can readily be seen (Figure 5b). 2C2P provides highly efficient excitation of tdKatushka2 (Figure 2), a fluorescent protein with exceptional brightness ~100 GM[11]. Excitation of tdKatushka2 is not easily accessible to standard Ti:S lasers due to its peak 2PE cross-section at 1100 nm. Even when compared with 1C2P excitation at 1055 nm, the 2C2P excitation has 40% higher signal level throughout the spheroid (Figure 5c). A number of other bright far-red fluorescent proteins are desirable for intravital microscopy, but cannot be efficiently excited by either ytterbium-based lasers or Ti:S lasers. Far-red fluorescent proteins such as mCardinal[12], mNeptune[32], and mKate2[10], all have peak 2PE cross-sections within 10 nm of the effective 2C2P excitation wavelength of 1140 nm (Figure 2). For these recently developed far-red fluorescent proteins, 2C2P at 1140 nm provides on average a 90% signal increase over 1C2P at 1055 nm (Supplementary Fig. S5). When comparing 2C2P at 1140 nm with 1C2P at 1240 nm, the signal level is still 42% higher averaged over all fluorophores. The benefit with this system is that near optimal excitation of far-red proteins can be achieved, while still maintaining direct excitation at 1055 and 1240 nm.

Although this laser system is optimized for efficient excitation of far-red fluorophores, we also demonstrate that blue emitting fluorophores can be excited at these longer wavelengths through two-color three-photon excitation (2C3P). While 2C2P has been demonstrated as early as 1996[33], and by several others[20,34], to our knowledge this is the first demonstration of 2C3P imaging. Using two-color excitation, the sample of Hoechst 33342 stained cells shows a power dependence (Figure 5d) with a slope of 3.04 ± 0.03 on a log-log scale, indicating a three-photon absorption process. We verify that this process is purely three-photon by performing the same experiment using only 1055 nm

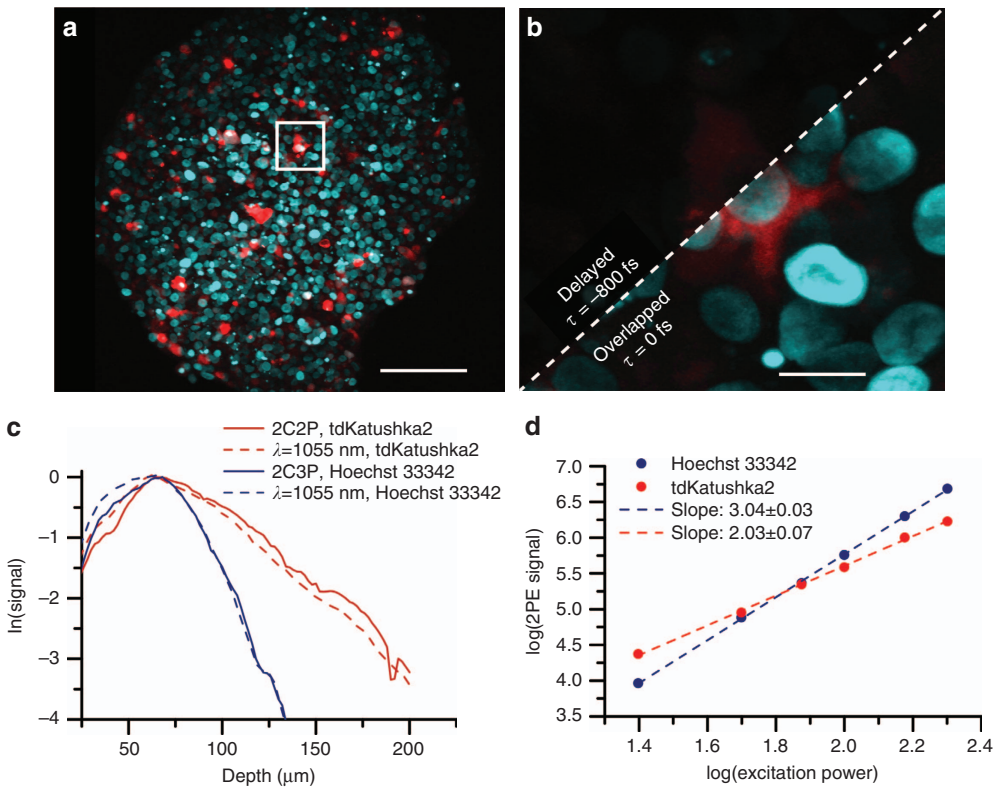

Figure 5 Two-color three-photon excitation of spheroids (**a**) Maximum intensity projection of a 200 μm thick spheroid with MCF-10A cells expressing tdKatushka2 (red) in vasodilator-stimulated phosphoprotein (VASP), and nuclei labelled with Hoechst 33342 (blue). Scale bar is 80 μm. (**b**) A 10 μm thick maximum intensity projection at 100 μm depth. The image is a zoom in of the white boxed region from panel (a) showing the effect of pulse synchronization on signal. The scale bar is 10 μm. (**c**) Mean image signal level versus depth for both color channels, tdKatushka2 (red), and Hoechst33342 (blue), and both excitation regimes, two-color excitation (solid line), and fiber amplifier only (dashed line). (**d**) Signal dependence versus excitation power for Hoechst 33342 (blue), and tdKatushka2 (red), using two-color excitation. tdKatushka2 undergoes two-photon excitation, while Hoechst33342 undergoes two-color three-photon excitation.

excitation, and also recover a slope of 3 (Supplementary Fig. S6). Direct (one-color) excitation accounts for approximately 40% of the signal from Hoechst 33342 (Figure 4c), so the remaining 60% of the signal can be inferred to be the product of 2C3P excitation. It should be noted that the signal increase from overlapping the two pulses could possibly contain some additional direct (1C3P) components, and the selection rules are certainly different between the two excitation processes, which could account for some signal variation. Nevertheless, the dramatic increase in signal when overlapped is likely due, in some part, to 2C3P excitation. The effective wavelengths for 2C3P take the form of $\lambda_{3a}=3/(2/\lambda_1+1/\lambda_2)$, and $\lambda_{3b}=3/(1/\lambda_1+2/\lambda_2)$, which enable four discrete energy transitions (1055, 1110, 1171 and 1240 nm in our system), as opposed to three with 2C2P. Additionally, 2C3P offers an even more confined focus due to third-order dependence on excitation intensity[35]. Considering these benefits, we predict potentially novel future applications of 2C3P.

Two-color excitation of cortical vasculature *in vivo*

Two-color two-photon microscopy is demonstrated *in vivo* with a series of stacks recorded in the same region in the brain of an adult live mouse, under three different excitation regimes (1) 2C2P $\tau=0$ fs, (2) 1C2P $\lambda=1055$ nm and (3) 2C2P $\tau=-600$ fs. The total excitation power at each plane was kept constant for each regime, with 20 mW for surface level imaging, and a maximum of 150 mW at depths beyond 400 μm. The microscope inefficiency accounts for the low maximum power at the back aperture, relative to each laser's raw output (>300 mW). Experimental conditions such as frame averaging, detector gain, and pixel dwell time were constant across all experimental regimes (Materials and methods section in Supplementary Information).

Texas Red is selected as a vasculature label for its high 2PE cross section at the 2C2P effective wavelength of 1140 nm. Verification that Texas Red is undergoing two-photon absorption was found through power dependence controls at both excitation wavelengths (Supplementary Fig. S7). The relative brightness of Texas Red is almost twice as high at 1140 nm compared to 1055 nm[36], although it has not been characterized out to 1240 nm. With 2C2P overlapped pulses ($\tau=0$ fs) a depth of 960 μm was reached (Figure 6a). For the other two excitation regimes, a depth of only 800 μm can be achieved before the signal is too low to be detected (Supplementary Fig. S8). Incidentally, an imaging depth of ~800 μm in the brain was previously reported by our group with Texas Red using a 1060 nm fiber oscillator[37]. The effect of 2C2P allows for 20% deeper imaging than with the fiber amplifier alone, by virtue of the longer wavelength excitation, and better matched 2PE cross-section to Texas Red. To confirm that the improved signal is from 2C2P and not from direct 1240 nm excitation, a control stack was recorded with delayed pulses ($\tau=-600$ fs). The effect of pulse delay dramatically reduces the signal-to-background ratio (SBR) and resulting image quality (Figure 6b). The SBR calculated using 2C2P ($\tau=0$ fs) at a depth of 945 μm was

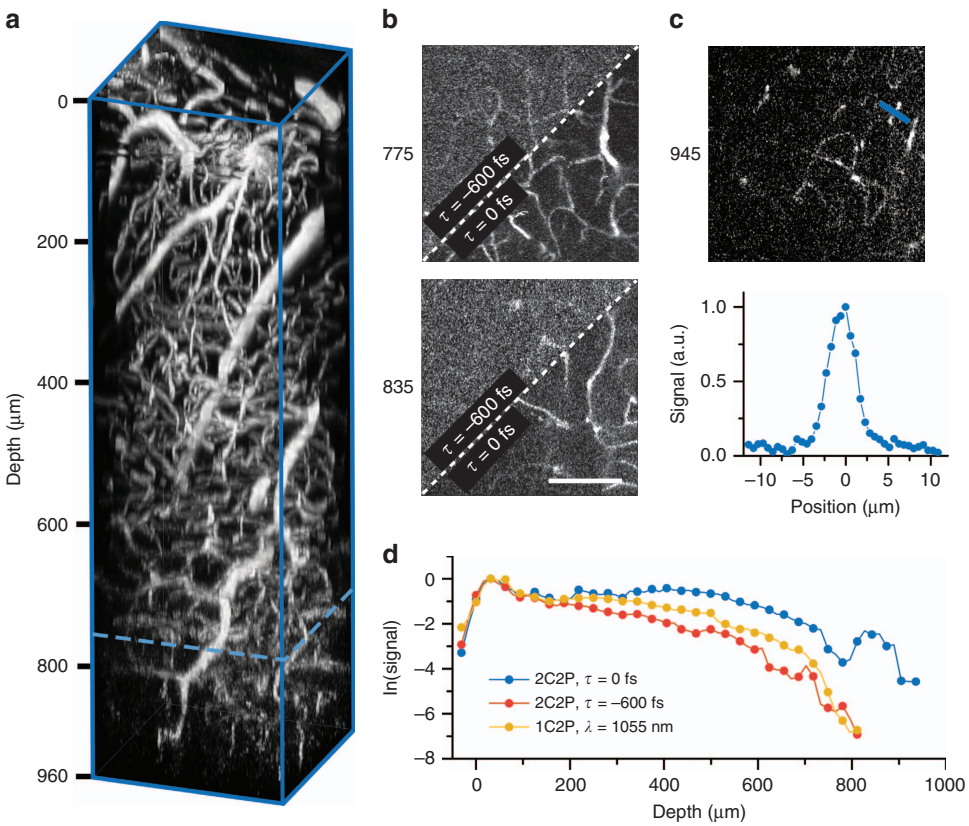

Figure 6 Deep *in vivo* microscopy with two-color excitation (**a**) Three dimensional reconstruction of a vascular images taken with two-color two-photon excitation ($\lambda_1=1055$ nm, $\lambda_2=1240$ nm) in the brain of an adult mouse. The field of view is 300 μm and the stack depth is 960 μm. The dotted blue line is the approximate depth limit of 1C2P ($\lambda=1055$ nm). (**b**) 2D plane maximum intensity projections of 20 μm thickness at 775 and 835 μm deep. The upper left section of each image shows the signal from 2C2P with pulses delayed $\tau=-600$ fs, while the bottom right section shows the signal acquired with overlapped pulses, $\tau=0$ fs. (**c**) Maximum intensity projection of five images over a 20 μm thickness taken with overlapped 2C2P excitation at a mean depth of 945 μm. The blue line denotes the region where a line profile is displayed in the lower panel. The signal to background ratio calculated from the line profile is 17. (**d**) Natural logarithm of the mean signal level versus depth. Scale bar, 100 μm.

doi:10.1038/lsa.2017.95

found to be 17 (Figure 6c), which is consistent with previous deep imaging demonstrations using longer wavelength excitation[15]. By quantifying the signal at each depth for all three excitation regimes, we find that 2C2P offers an average of 3× more signal for images beyond 400 μm compared with the fiber amplifier alone (Figure 6d). However, the signal decay rate (slope = −0.006) is approximately the same for all three excitation regimes, implying that the fundamental imaging depth is not necessarily improved with 2C2P, just the signal level for a given excitation power.

Here we show that an imaging depth of nearly 1 mm can be achieved through 2C2P excitation of Texas Red in the cortical vasculature of a live mouse. The imaging depth with 2C2P is a 20% increase over using 1055 nm excitation alone. We also note that 1C2P excitation at 1055 nm is not fundamentally limited to shallower imaging depths, as we show that when matched with a better fluorophore, such as tdTomato, it is possible to image neural structure down to 1 mm in a live mouse brain (Supplementary Fig. S9). The described dual output source allows for optimal excitation of most fluorophores over the range of 1000–1300 nm, making it a valuable tool for efficient multicolor imaging *in vivo*.

Two-color two-photon excitation is a relatively new approach for multicolor microscopy, as turnkey synchronized dual output sources have only become commercially available within the past few years. Yet, currently these dual output sources are hardly attainable for the typical biological imaging laboratory, primarily due to their cost and limited availability. For this reason, very few reports have detailed any form of 2C2P tissue microscopy. While a few reports have focused on the photophysical properties of 2C2P[33,34], and one demonstrates 2C2P with fluorescence lifetime imaging[38], only one group has explored its use for multicolor imaging in tissue samples[20].

The prior demonstrations of 2C2P for tissue microscopy have used an OPO and the residual Ti:S pump as the secondary excitation laser to achieve 2C2P near ~950 nm. But this approach is restricted to short wavelengths, since the Ti:S needs to be tuned to <880 nm for efficient operation of the OPO, which results in restricted penetration depth in scattering biological samples[16]. Furthermore, the Ti:S/OPO combination would not be practical for 2C2P excitation at an effective wavelength near 1140 nm because the OPO would need to be tuned to >1900 nm where its output power would be very low and suffer from water absorption (assuming the Ti:S pump is at 800 nm). The OPO alone can excite at 1140 nm through one-color two-photon excitation, but this eliminates the benefits of two-color excitation, described by Mahou *et al.* for multicolor imaging. Therefore, while 2C2P imaging has been demonstrated before, the novelty of our work is that it provides a new excitation source for 2C2P imaging that extends beyond the current capabilities of Ti:S/OPO two-color excitation. In this report, we show that 2C2P with a diamond Raman laser is not only feasible for *in vivo* microscopy, but is often advantageous when compared with 1C2P. With 2C2P excitation at 1140 nm we demonstrate a 90% increase in signal for many common far-red fluorescent proteins, and 20% deeper imaging with Texas Red when compared with 1C2P excitation at 1055 nm.

Other than commercial laser sources for *in vivo* microscopy, several custom solutions have been developed by others. An output of 1250 nm was achieved by nonlinear generation in fiber with a 1070 nm seed[39]. A Cr:forsterite laser tunable over 1220–1270 nm has also been used for harmonic generation microscopy[40]. In addition, a synchronously pumped fiber-based Raman laser has been demonstrated[41]. However, these approaches have significant limitations. For nonlinear generation in fiber, the pulse energy was limited to only 0.6 nJ which is not sufficient for *in vivo* applications. Furthermore, the nonlinear generation process is highly inefficient, making it difficult to use the seed laser as a second output for 2C2P. Cr:forsterite lasers suffer from alignment and implementation challenges because of their relatively complicated cavity and requirement for active cooling. Furthermore, they are not compatible with 2C2P, due to continuous wave pumping. The fiber-based Raman source demonstrated by Churin *et al.* could potentially be used for two-color excitation. However, with a Raman spectrum shifted only 50 nm (from 1030 to 1080 nm), the benefit of accessing excitation of different fluorophores is diminished and cannot compete directly in terms of efficient far-red fluorophore excitation. On the other hand, our diamond Raman laser, with a Stokes shift of 185 nm, enables efficient excitation of far-red fluorophores over a broad spectral range (Figure 2).

While it is clear that in the past two decades there has been no robust or cost effective means for generating two synchronized outputs needed to perform 2C2P, there are still a number of studies investigating the potential benefits of the approach. Several theoretical investigations have proposed 2C2P as a means to achieve superresolution[42,43], or to reduce background noise[44–46]. With the described laser system, some of these theorized studies could be experimentally verified. In addition, with 2C3P excitation described herein, it could be possible to achieve enhanced results because of the higher order dependence on excitation intensity. On the basis of the simplicity of the fiber-pumped diamond Raman laser design (Supplementary Figs. S10, S11), we see no challenge for other groups to adopt this as a robust platform for development of 2C2P or 2C3P applications.

The results demonstrate that *in vivo* imaging is possible even with a relatively low power of 150 mW at depth. With the current level of excitation power, the images at depth are most likely power limited rather than limited by tissue scattering. When going beyond 960 μm the signal falls off dramatically, whereas the background remains relatively constant. Accounting for the inefficiencies in the microscope, some improvement could be made to increase throughput within the 1000–1300 nm excitation range, although it would likely be a modest improvement ~20%. However, there is no fundamental issue with scaling the output power of the diamond Raman laser up to Watt levels with higher pump power[23,25]. Increasing pump power has the added advantage of increased nonlinearity in the diamond, which broadens the Raman output spectrum, resulting in an even more compressible pulse. With additional dispersion compensating elements in the cavity it is possible to reach 25 fs pulse-widths from a diamond Raman laser[47]. A 25 fs pulse could improve signal at depth, so long as appropriate measures are taken to compensate for dispersion. Although our implementation of a diamond Raman laser offers no wavelength tuning, diamond Raman lasers, in principle, are continuously tunable dependent on pump input[48]. With the addition of a tunable pump source along with 2C2P it could be possible to offer an even greater range and continuity of excitation wavelengths.

CONCLUSIONS

Many far-red dyes compatible with deep *in vivo* microscopy of vasculature have been characterized for peak 2PE cross-sections between 1200 and 1300 nm[49], whereas most far-red fluorescent proteins compatible with neuron labelling have a peak 2PE cross-section in the range of 1000–1150 nm[11]. When using a single output laser source, even a tunable one, there will always be a tradeoff in excitation efficiency between multicolor labels, which in turn restricts the fundamental imaging depth with either, or both labels. Whereas, 2C2P with the fiber amplifier pumped diamond Raman laser allows for highly efficient excitation of both vascular and neural labelling strategies, through its near complete coverage of the

1000–1300 nm excitation range. At $50,000 for all components (Supplementary Tables S1 and S2), the cost of the system is an order of magnitude less than commercial dual output lasers, and nearly half that of a typical Ti:S laser. We expect the fiber-pumped diamond Raman laser to be a highly desirable alternative to the OPO for simultaneous multicolor imaging *in vivo*. In addition, this dual output laser system is a critical enabling tool to explore the future possibilities of 2C2P and 2C3P excitation microscopy.

CONFLICT OF INTEREST

The authors declare no conflict of interest.

ACKNOWLEDGEMENTS

This study has been supported by the National Institutes of Health (NS082518, CA193038, NS078791 and EB011556), the American Heart Association (14EIA18970041), and Cancer Prevention Research Institute of Texas (RR160005). We thank Dr Amy Brock for providing the MCF-10A cell line. tdKatushka2-VASP-5 was a gift from Michael Davidson (Addgene plasmid # 56049).

1 Zipfel WR, Williams RM, Webb WW. Nonlinear magic: multiphoton microscopy in the biosciences. *Nat Biotechnol* 2003; **21**: 1369–1377.
2 Helmchen F, Denk W. Deep tissue two-photon microscopy. *Nat Methods* 2005; **2**: 932–940.
3 Stosiek C, Garaschuk O, Holthoff K, Konnerth A. *In vivo* two-photon calcium imaging of neuronal networks. *Proc Natl Acad Sci USA* 2003; **100**: 7319–7324.
4 Tischbirek C, Birkner A, Jia HB, Sakmann B, Konnerth A. Deep two-photon brain imaging with a red-shifted fluorometric Ca^{2+} indicator. *Proc Natl Acad Sci USA* 2015; **112**: 11377–11382.
5 Dana H, Mohar B, Sun Y, Narayan S, Gordus A *et al.* Sensitive red protein calcium indicators for imaging neural activity. *eLife* 2016; **5**: e12727.
6 Sakadžić S, Roussakis E, Yaseen MA, Mandeville ET, Srinivasan VJ *et al.* Two-photon high-resolution measurement of partial pressure of oxygen in cerebral vasculature and tissue. *Nat Methods* 2010; **7**: 755–759.
7 Lecoq J, Parpaleix A, Roussakis E, Ducros M, Houssen YG *et al.* Simultaneous two-photon imaging of oxygen and blood flow in deep cerebral vessels. *Nat Med* 2011; **17**: 893–898.
8 Kazmi SMS, Salvaggio AJ, Estrada AD, Hemati MA, Shaydyuk NK *et al.* Three-dimensional mapping of oxygen tension in cortical arterioles before and after occlusion. *Biomed Opt Express* 2013; **4**: 1061–1073.
9 Prakash R, Yizhar O, Grewe B, Ramakrishnan C, Wang N *et al.* Two-photon optogenetic toolbox for fast inhibition, excitation and bistable modulation. *Nat Methods* 2012; **9**: 1171–1179.
10 Shcherbo D, Murphy CS, Ermakova GV, Solovieva EA, Chepurnykh TV *et al.* Far-red fluorescent tags for protein imaging in living tissues. *Biochem J* 2009; **418**: 567–574.
11 Drobizhev M, Makarov NS, Tillo SE, Hughes TE, Rebane A. Two-photon absorption properties of fluorescent proteins. *Nat Methods* 2011; **8**: 393–399.
12 Chu J, Haynes RD, Corbel SY, Li PP, González-González E *et al.* Non-invasive intravital imaging of cellular differentiation with a bright red-excitable fluorescent protein. *Nat Methods* 2014; **11**: 572–578.
13 Dunn AK, Wallace VP, Coleno M, Berns MW, Tromberg BJ. Influence of optical properties on two-photon fluorescence imaging in turbid samples. *Appl Opt* 2000; **39**: 1194–1201.
14 Oheim M, Beaurepaire E, Chaigneau E, Mertz J, Charpak S. Two-photon microscopy in brain tissue: parameters influencing the imaging depth. *J Neurosci Methods* 2001; **111**: 29–37.
15 Kobat D, Horton NG, Xu C. *In vivo* two-photon microscopy to 1.6-mm depth in mouse cortex. *J Biomed Opt* 2011; **16**: 106014.
16 Horton NG, Wang K, Kobat D, Clark CG, Wise FW *et al. In vivo* three-photon microscopy of subcortical structures within an intact mouse brain. *Nat Photonics* 2013; **7**: 205–209.
17 Entenberg D, Wyckoff J, Gligorijevic B, Roussos ET, Verkhusha VV *et al.* Setup and use of a two-laser multiphoton microscope for multichannel intravital fluorescence imaging. *Nat Protoc* 2011; **6**: 1500–1520.
18 Yokoyama H, Tsubokawa H, Guo HC, Shikata J, Sato K *et al.* Two-photon bioimaging utilizing supercontinuum light generated by a high-peak-power picosecond semiconductor laser source. *J Biomed Opt* 2007; **12**: 054019.
19 Brenner MH, Cai DW, Swanson JA, Ogilvie JP. Two-photon imaging of multiple fluorescent proteins by phase-shaping and linear unmixing with a single broadband laser. *Opt Express* 2013; **21**: 17256–17264.
20 Mahou P, Zimmerley M, Loulier K, Matho KS, Labroille G *et al.* Multicolor two-photon tissue imaging by wavelength mixing. *Nat Methods* 2012; **9**: 815–818.
21 Mahou P, Vermot J, Beaurepaire E, Supatto W. Multicolor two-photon light-sheet microscopy. *Nat Methods* 2014; **11**: 600–601.
22 Spence DJ, Granados E, Mildren RP. Mode-locked picosecond diamond Raman laser. *Opt Lett* 2010; **35**: 556–558.
23 Murtagh M, Lin JP, Mildren RP, McConnell G, Spence DJ. Efficient diamond Raman laser generating 65 fs pulses. *Opt Express* 2015; **23**: 15504–15513.
24 Trägårdh J, Murtagh M, Robb G, Parsons M, Lin J *et al.* Two-color, two-photon imaging at long excitation wavelengths using a diamond Raman laser. *Microsc Microanal* 2016; **22**: 803–807.
25 Warrier AM, Lin JP, Pask HM, Mildren RP, Coutts DW *et al.* Highly efficient picosecond diamond Raman laser at 1240 and 1485 nm. *Opt Express* 2014; **22**: 3325–3333.
26 Kruglov VI, Peacock AC, Harvey JD, Dudley JM. Self-similar propagation of parabolic pulses in normal-dispersion fiber amplifiers. *J Opt Soc Am B* 2002; **19**: 461–469.
27 Dudley JM, Finot C, Richardson DJ, Millot G. Self-similarity in ultrafast nonlinear optics. *Nat Phys* 2007; **3**: 597–603.
28 Limpert J, Schreiber T, Clausnitzer T, Zöllner K, Fuchs H-J *et al.* High-power femtosecond Yb-doped fiber amplifier. *Opt Express* 2002; **10**: 628–638.
29 Papadopoulos DN, Zaouter Y, Hanna M, Druon F, Mottay E *et al.* Generation of 63 fs 4.1 MW peak power pulses from a parabolic fiber amplifier operated beyond the gain bandwidth limit. *Opt Lett* 2007; **32**: 2520–2522.
30 Deng YJ, Chien C-Y, Fidric BG, Kafka JD. Generation of sub-50 fs pulses from a high-power Yb-doped fiber amplifier. *Opt Lett* 2009; **34**: 3469–3471.
31 Millard AC, Fittinghoff DN, Squier JA, Müller M, Gaeta AL. Using GaAsP photodiodes to characterize ultrashort pulses under high numerical aperture focusing in microscopy. *J Microsc* 1999; **193**: 179–181.
32 Lin MZ, McKeown MR, Ng HL, Aguilera TA, Shaner NC *et al.* Autofluorescent proteins with excitation in the optical window for intravital imaging in mammals. *Chem Biol* 2009; **16**: 1169–1179.
33 Lakowicz JR, Gryczynski I, Malak H, Gryczynski Z. Two-color two-photon excitation of fluorescence. *Photochem Photobiol* 1996; **64**: 632–635.
34 Quentmeier S, Denicke S, Ehlers J-E, Niesner RA, Gericke KH. Two-color two-photon excitation using femtosecond laser pulses. *J Phys Chem B* 2008; **112**: 5768–5773.
35 Hell SW, Bahlmann K, Schrader M, Soini A, Malak HM *et al.* Three-photon excitation in fluorescence microscopy. *J Biomed Opt* 1996; **1**: 71–74.
36 Bestvater F, Spiess E, Stobrawa G, Hacker M, Feurer T *et al.* Two-photon fluorescence absorption and emission spectra of dyes relevant for cell imaging. *J Microsc* 2002; **208**: 108–115.
37 Perillo EP, McCracken JE, Fernée DC, Goldak JR, Medina FA *et al.* Deep *in vivo* two-photon microscopy with a low cost custom built mode-locked 1060 nm fiber laser. *Biomed Opt Express* 2016; **7**: 324–334.
38 Robinson T, Valluri P, Kennedy G, Sardini A, Dunsby C *et al.* Analysis of DNA binding and nucleotide flipping kinetics using two-color two-photon fluorescence lifetime imaging microscopy. *Anal Chem* 2014; **86**: 10732–10740.
39 Domingue SR, Bartels RA. Three-photon excitation source at 1250 nm generated in a dual zero dispersion wavelength nonlinear fiber. *Opt Express* 2014; **22**: 30777–30785.
40 Sun C–K, Chu SW, Chen SY, Tsai TH, Liu TM *et al.* Higher harmonic generation microscopy for developmental biology. *J Struct Biol* 2004; **147**: 19–30.
41 Churin D, Olson J, Norwood RA, Peyghambarian N, Kieu K. High-power synchronously pumped femtosecond Raman fiber laser. *Opt Lett* 2015; **40**: 2529–2532.
42 Hell SW. Improvement of lateral resolution in far-field fluorescence light microscopy by using two-photon excitation with offset beams. *Opt Commun* 1994; **106**: 19–24.
43 Xiao FR, Wang GY, Xu ZZ. Superresolution in two-color excitation fluorescence microscopy. *Opt Commun* 2003; **228**: 225–230.
44 Cambaliza MO, Saloma C. Advantages of two-color excitation fluorescence microscopy with two confocal excitation beams. *Opt Commun* 2008; **184**: 25–35.
45 Blanca CM, Saloma C. Two-color excitation fluorescence microscopy through highly scattering media. *Appl Opt* 2001; **40**: 2722–2729.
46 Wang C, Qiao LL, Mao ZL, Cheng Y, Xu ZZ. Reduced deep-tissue image degradation in three-dimensional multiphoton microscopy with concentric two-color two-photon fluorescence excitation. *J Opt Soc Am B* 2008; **25**: 976–982.
47 Lin JP, Spence DJ. 25.5 fs dissipative soliton diamond Raman laser. *Opt Lett* 2016; **41**: 1861–1864.
48 Sabella A, Piper JA, Mildren RP. Diamond Raman laser with continuously tunable output from 3.38 to 3.80 μm. *Opt Lett* 2014; **39**: 4037–4040.
49 Kobat D, Durst ME, Nishimura N, Wong AW, Schaffer CB *et al.* Deep tissue multiphoton microscopy using longer wavelength excitation. *Opt Express* 2009; **17**: 13354–13364.

Supplementary Information for this article can be found on the *Light: Science & Applications*' website (http://www.nature.com/lsa).